

## Supporting information

### **The $K_{sp}$ gap enabled precipitation transformation reactions from transition metal hydroxides to sulfides for alkali metal ion storage**

Qianrui Zhao,<sup>a</sup> Zhiwen Tang,<sup>a</sup> Yuede Pan,<sup>\*a,b</sup> Jingjing Han,<sup>a</sup> Jinbiao Yang,<sup>a</sup> Yongqiang Guo,<sup>a</sup> Xiangqian Lai,<sup>a</sup> Zhewei Yang,<sup>a</sup> Gang Li<sup>\*a</sup>

<sup>a</sup> *Institute of Energy Innovation, College of Materials Science and Engineering, Taiyuan University of Technology, Taiyuan 030024, China.*

<sup>b</sup> *Key Laboratory of Advanced Energy Materials Chemistry (Ministry of Education), College of Chemistry, Nankai University, Tianjin 300071, China.*

\*Corresponding authors:

panyuede@tyut.edu.cn (Y. Pan);

ligang02@tyut.edu.cn (G. Li);

Contents: Fig. S1–S5; Table S1

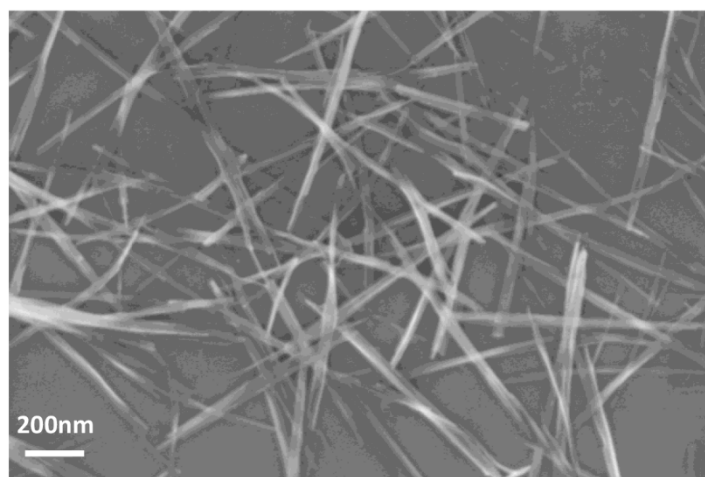


Fig. S1. Scanning electron microscope (SEM) image of Cu(OH)<sub>2</sub> nanowires.

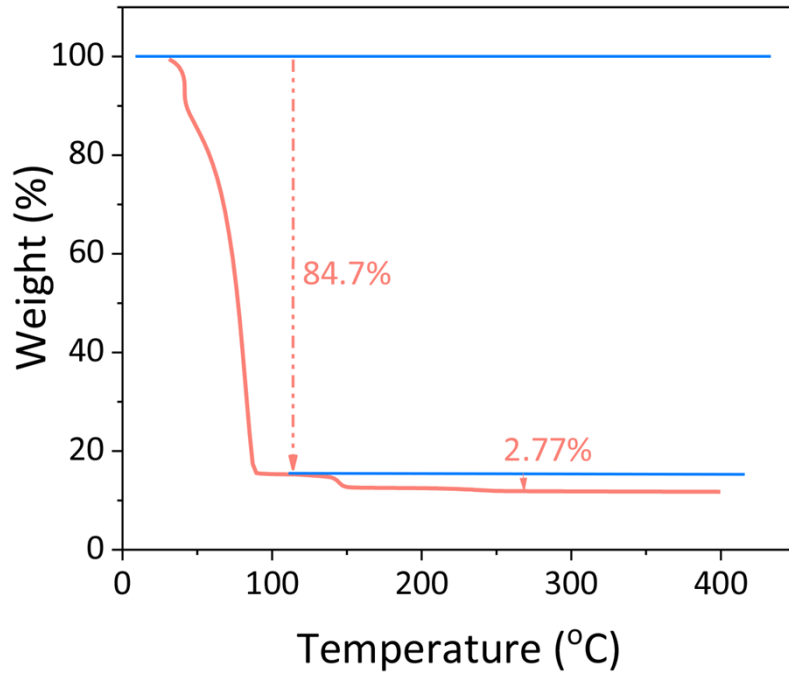


Fig. S2. Thermogravimetric (TG) curve of Cu(OH)<sub>2</sub> nanowires.

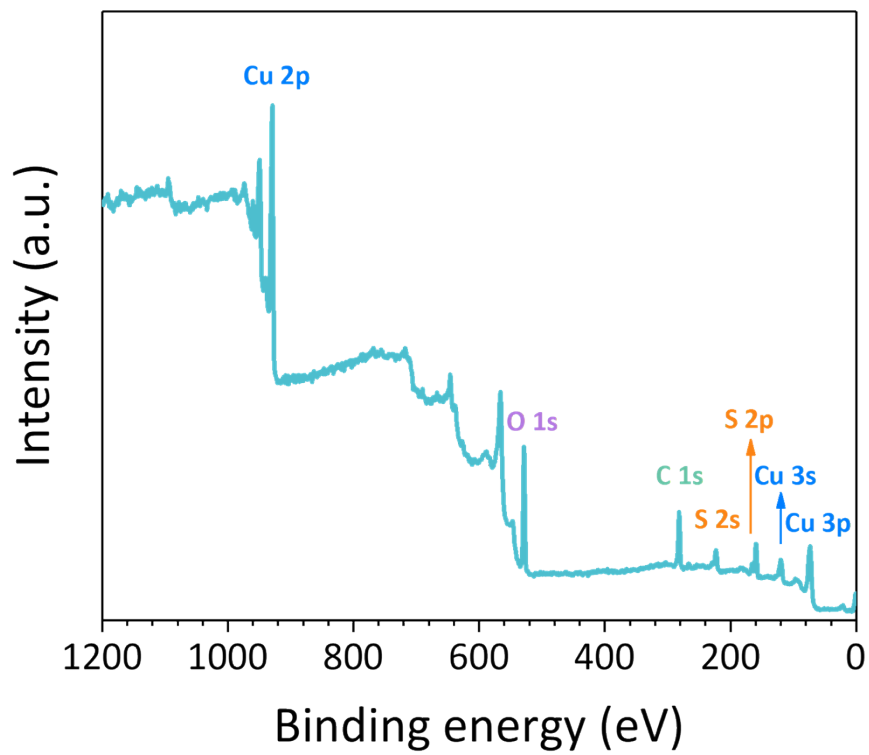


Fig. S3. X-ray photoelectron spectroscopy (XPS) curve of the CuS nanomaterial derived from  $\text{Cu}(\text{OH})_2$  nanowires.

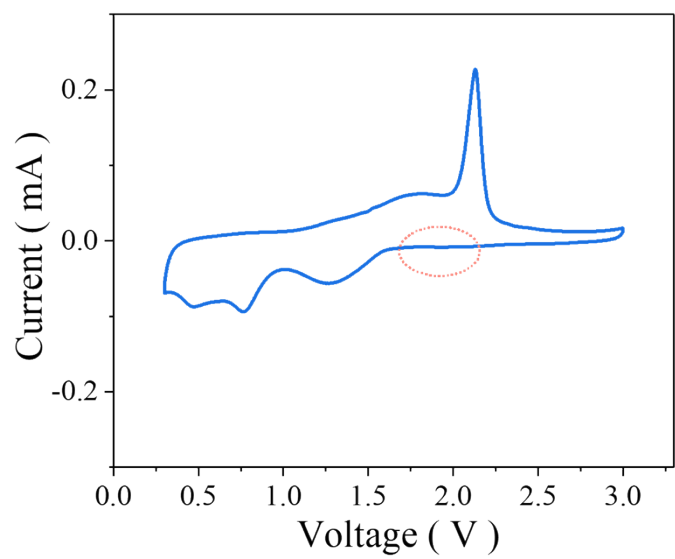


Fig. S4. CV curve for the fifth cycle of the SIB at a sweep rate of  $0.1 \text{ mV s}^{-1}$ .

Table S1. The chemical reaction equations corresponding to the redox peak of the cyclic voltammetry curves for the alkali metal ion batteries.

	Peak voltage		Redox equation	Process	
	1 <sup>st</sup> cycle	2 <sup>nd</sup> cycle			
reduction peak	SIB	1.91V	1.94	$\text{CuS} + y\text{Na}^+ + ye^- \rightarrow \text{Na}_y\text{CuS} (y < 0.5)$ (Irreversible reaction)	R1
		1.41V	1.41	$\text{Na}_y\text{CuS} + (x-y)\text{Na}^+ + (x-y)e^- \rightarrow \text{Na}_x\text{CuS}$ ( $0.5 < x < 1$ )	
		1.11	-	Formation of SEI film	
		0.73V	0.73	$2\text{Na}_x\text{CuS} + (2-2x)\text{Na}^+ + (2-2x)e^- \rightarrow \text{Cu}_2\text{S} + \text{Na}_2\text{S}$	R2
		0.41V	0.38	$\text{Cu}_2\text{S} + 2\text{Na}^+ + 2e^- \rightarrow 2\text{Cu} + \text{Na}_2\text{S}$	R3
	LIB	2.03V	2.08	$\text{CuS} + y\text{Li}^+ + ye^- \rightarrow \text{Li}_y\text{CuS}$	R1
		1.58V	1.60	$\text{Li}_y\text{CuS} + (x-y)\text{Li}^+ + (x-y)e^- \rightarrow \text{Li}_x\text{CuS}$	
		1.20V	1.24	$2\text{Li}_x\text{CuS} + (2-2x)\text{Li}^+ + (2-2x)e^- \rightarrow \text{Cu}_2\text{S} + \text{Li}_2\text{S}$	R2
		0.85V	0.85	$\text{Cu}_2\text{S} + 2\text{Li}^+ + 2e^- \rightarrow 2\text{Cu} + \text{Li}_2\text{S}$	R3
		PIB	1.76V	1.95	$\text{CuS} + x\text{K}^+ + xe^- \rightarrow \text{K}_x\text{CuS}$
1.20V	1.41				
0.83	-		Formation of SEI film		
		0.51V	0.51	$\text{K}_x\text{CuS} + (2-x)\text{K}^+ + (2-x)e^- \rightarrow \text{Cu} + \text{K}_2\text{S}$	R3
Oxidation peak	SIB	1.79V	1.79	$2\text{Cu} + \text{Na}_2\text{S} \rightarrow \text{Cu}_2\text{S} + 2\text{Na}^+ + 2e^-$	O1
		2.13V	2.13	$\text{Cu}_2\text{S} + \text{Na}_2\text{S} \rightarrow 2\text{Na}_x\text{CuS} + (2-2x)\text{Na}^+ + (2-2x)e^-$	O2
	LIB	1.87V	1.87	$2\text{Cu} + \text{Li}_2\text{S} \rightarrow \text{Cu}_2\text{S} + 2\text{Li}^+ + 2e^-$	O1
		2.06V	2.06	$\text{Cu}_2\text{S} + \text{Li}_2\text{S} \rightarrow 2\text{Li}_x\text{CuS} + (2-2x)\text{Li}^+ + (2-2x)e^-$	O2
		2.28V	2.28	$\text{Li}_x\text{CuS} \rightarrow \text{CuS} + x\text{Li}^+ + xe^-$	O3
	PIB	1.44V	1.44	$\text{Cu} + \text{K}_2\text{S} \rightarrow \text{K}_x\text{CuS} + (2-x)\text{K}^+ + (2-x)e^-$	O1
		2.00V	2.04		
		2.39V	2.45	$\text{K}_x\text{CuS} \rightarrow \text{CuS} + x\text{K}^+ + xe^-$	O3

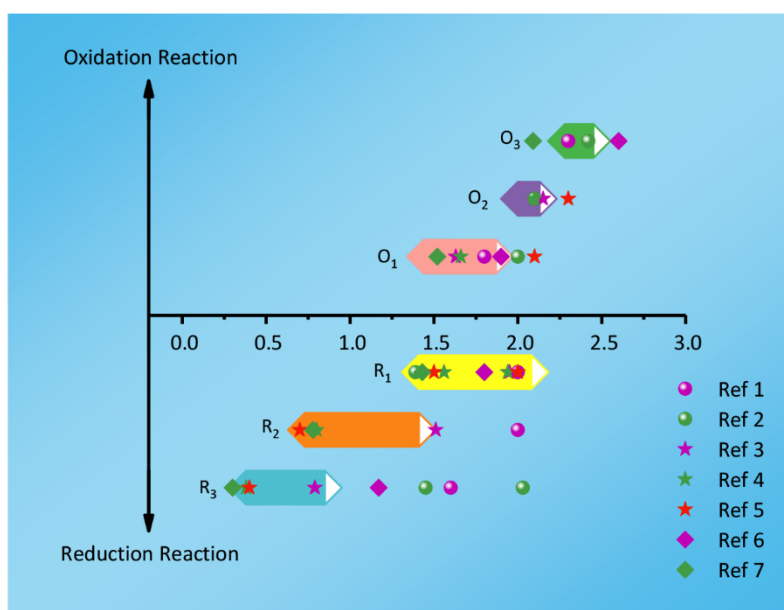


Fig. S5. Illustration of the peak voltage ranges for CuS storing Li<sup>+</sup>, Na<sup>+</sup>, or K<sup>+</sup> in literature.<sup>1-7</sup>

## References

1. Y. Li, Y. Zhang, Y. Wang, X. Li, Q. Zhang, H. Yan, X. Huang, H. Liu and Y. Zhang, Effect of ether-based electrolyte composition on the lithium storage performance of copper sulfide, *Electrochimica Acta*, 2020, **335**, 135662.
2. Y. h. Zhang, L. j. Xu, R. h. Liu, Y. c. Wang, S. h. Luo, Q. Wang and X. Liu, CuS nanoblocks embedded in the three-dimensional porous carbon as composite anode materials for high-performance lithium-ion battery, *Ionics*, 2021, **27**, 897-905.
3. Y. Hu, L. Zhang, J. Bai, F. Liu, Z. Wang, W. Wu, R. Bradley, L. Li, H. Ruan and S. Guo, Boosting High-Rate Sodium Storage of CuS via a Hollow Spherical Nanostructure and Surface Pseudocapacitive Behavior, *ACS Appl. Energy Mater.*, 2021, **4**, 8901-8909.
4. D. Yu, M. Li, T. Yu, C. Wang, Y. Zeng, X. Hu, G. Chen, G. Yang and F. Du, Nanotube-assembled pine-needle-like CuS as an effective energy booster for sodium-ion storage, *J. Mater. Chem. A*, 2019, **7**, 10619-10628.
5. Y. Xiao, D. Su, X. Wang, S. Wu, L. Zhou, Y. Shi, S. Fang, H.-M. Cheng and F. Li, CuS Microspheres with Tunable Interlayer Space and Micropore as a High-Rate and Long-Life Anode for Sodium-Ion Batteries, *Adv. Energy Mater.*, 2018, **8**, 1800930.
6. T. G. Nithya C Morphology oriented CuS nanostructures: Superior K-ion storage by surface enhanced pseudocapacitive effects, *Sustain. Energy Fuels*, 2020, **4**, 1-16.
7. X. Jia, E. Zhang, X. Yu and B. Lu, Facile Synthesis of Copper Sulfide Nanosheet@Graphene Oxide for the Anode of Potassium-Ion Batteries, *Energy Technol.*, 2019, **8**, 1900987.